

Analysis of lacunarity and scales of spatial homogeneity in IKONOS images of Amazonian tropical forest canopies

Yadvinder Malhi^{*}, Rosa María Román-Cuesta¹

Environmental Change Institute, Oxford University Centre for the Environment, South Parks Road, Oxford OX13QY, United Kingdom

Received 13 September 2006; received in revised form 19 November 2007; accepted 2 January 2008

Abstract

Extensive plot studies across Amazonia have demonstrated that there are large regional gradients in forest productivity and that the dynamics of the forests seem to have accelerated substantially in recent decades, with ensuing impacts on forest structure. Most of these sites are, however, one hectare plots nested within a heterogeneous landscape, and a clear need exists to understand the landscape and regional context of these studies. Remote sensing offers the potential to scale up from plot to higher landscape levels but it has proven complex to evaluate forest structure, and therefore biomass patterns in tropical areas, due to saturation, signal noises, and unclear relationships between reflectance values and structural properties, both for optical and radar systems. In this study, we explore the potential of a textural approach to detect landscape and regional variations in the structure of tropical forest canopies, as viewed from high resolution IKONOS satellite imagery. We used lacunarity analysis and a derived variable, the index of translational homogeneity (ITH), as a tool to search for structural and dynamic forest properties within and among different Amazonian landscapes. The main goals of this research were: (1) to examine the sensitivity and robustness of ITH analysis to details of the analysis procedure; (2) to explore the intra- and inter-regional textural properties of a variety of tropical forest canopies [Caxiuana, Manaus, Sinop, Santarem (Brazil), and Tambopata (Peru)], and (3) to relate textural properties derived from lacunarity to structural properties of the forest canopy, mainly crown size. Our results show how ITH and lacunarity analyses offer insights into the spatial distribution of structural properties of forest canopies, easily differentiating between *terra firme* forests and swamp forests. The studied forest canopies are self-similar on length-scales of 5–11 m, and show translational invariance on scales above 20 m (central and western Amazonia) and 30 m (eastern Amazonia) For a restricted range of solar elevation angles, the ITH appears to be determined mainly by the mean size of tree crowns, and by the fraction of large (shadow-generating) trees.

© 2008 Elsevier Inc. All rights reserved.

Keywords: Lacunarity; Forest structure; Rainforests; IKONOS; Amazon; Fractals; Heterogeneity

1. Introduction

Tropical forests are probably the least understood of the major terrestrial biomes. Their complexity comes primarily from their high diversity (100–300 tree species/hectare) and the preponderance of old-growth mixed-age stands, in contrast to current temperate and boreal forests. These features, together with logistical difficulties of access, make it a challenge to understand tropical forest dynamics and structure at appropriate scales. Such knowledge is essential however if we are to understand the role

of tropical forests in the global carbon cycle, and the impact of atmospheric change on tropical forest structure, dynamics and diversity. In our recent work, we have compiled and established an extensive dataset of forest plots across Amazonia (Malhi et al., 2002) and have demonstrated, amongst other things, that there are large regional gradients in forest productivity (Malhi et al., 2004), and that the dynamics of the forests appear to have accelerated substantially in recent decades (Phillips et al., 2004) with ensuing impacts on forest structure. However, most of our sites are 1 ha plots nested within a heterogeneous landscape. There is clearly a need to understand the landscape and regional context of these study sites.

Satellite remote sensing provides the potential to scale from plot level studies to the regional level, and a variety of techniques and approaches have provided successful measurements of forest

^{*} Corresponding author. Tel.: +44 1865 271913; fax: +44 1865271929.

E-mail addresses: yadvinder.malhi@ouce.ox.ac.uk (Y. Malhi), rosa.roman@ouce.ox.ac.uk (R.M. Román-Cuesta).

¹ Tel.: +44 1865 275866; fax: +44 1865271929.

structure at different scales (Wulder & Franklin, 2004). However, some of these techniques can be highly demanding in terms of software, specialized training and costs of the high resolution images, such as IKONOS. Less specialized approaches, such as spectral analysis from more accessible images (e.g. Landsat data), frequently encounter problems when identifying regional variations in tropical forest biomass due to signal saturation in high biomass forests (Huete et al., 2002; Toan et al., 2004). The production of wood (the main long-term C stock) is usually determined by estimating photosynthesis from canopy radiometric properties. This also poses difficulties as the proportion of photosynthesis that is allocated to wood, and the residence time of that wood may be highly variable (Malhi et al., 2004). Hence, there is currently no easy and accessible method to determine tropical forest biomass and wood productivity from reflectance data. An alternative approach would be to rely on non-spectral properties of remote sensing, such as canopy structural and textural factors. Textural measures of tropical forest stands have become a popular approach to search for spatio-temporal variations of forest structure and dynamics. For example, a pan-tropical analysis of temporal trends in the lacunarity (a measure of textural properties, defined below) of tropical forest canopies (Weishampel et al., 2001) suggested that the lacunarity of tropical forest canopies (as seen in Landsat images) was increasing over time. Also, Frazer et al. (2005) found a strong relationship between the magnitude of lacunarity and estimates of canopy cover and gap fraction, across spatial scales. Weishampel et al. (2001) suggest that their results may be a signal of the wide spread acceleration of forest dynamics as suggested by a network of forest plots in Amazonia (Lewis et al., 2004; Phillips et al., 2004). It remains very unclear exactly what aspects of forest structure are captured by lacunarity, however, and hence interpretation of the Weishampel et al. (2001) results in terms of forest structure remains difficult.

Moreover, problems arise with the spatial resolution of the satellites (e.g. ca. 80 m for Landsat MSS and 30 m for Landsat TM), which cannot resolve tree crowns, the primary indicators of tree size and forest structure. The recent advent of commercially available high resolution satellite data like IKONOS and Quickbird with panchromatic resolutions of ≤ 1 m has now opened the possibility for direct analysis of

tropical forest crown structure, marking the advent of a new field of “space forestry” (Palace et al., in press). Lacunarity appears to have some potential to assist in the characterization of forest structure (in particular crown size and gap frequency), and of spatial and temporal trends in the structure. In this paper we explore this potential to detect landscape and regional variations in the structure of tropical forest canopies as viewed from high resolution satellite imagery, with the ultimate goal of inferring biomass properties from those observed forest patterns.

1.1. Aims

We explore the potential of lacunarity-derived texture indices to yield information about tropical forest canopy structure from high-resolution satellite images. Our specific aims are to:

1. Examine the sensitivity and robustness of lacunarity analysis to details of the analysis procedure.
2. Explore the intra- and inter-landscape textural properties of a variety of tropical forest canopies, with particular attention to the characterization of scales of spatial homogeneity or translational invariance.
3. Relate textural properties derived from lacunarity to structural properties of the forest canopy.

1.2. Definition of lacunarity

Lacunarity is a concept introduced by Mandelbrot (1983) to describe the distribution of the gap sizes in a fractal sequence. Geometric objects appear more lacunar if they contain a wide range of gap sizes. As a result, lacunarity can be thought as a measure of ‘gappiness’ or ‘hole-iness’ of a geometric structure. Gefen et al. (1983) gave a more precise definition: lacunarity measures the deviation of a geometric object, such as a fractal, from translational invariance. A geometric object has translational invariance at a particular scale if the statistical properties of the object at that scale do not vary with position on that object. Translational variance is highly scale-dependent: objects that are heterogeneous at small scales can be quite homogeneous when examined at larger scales or vice versa.

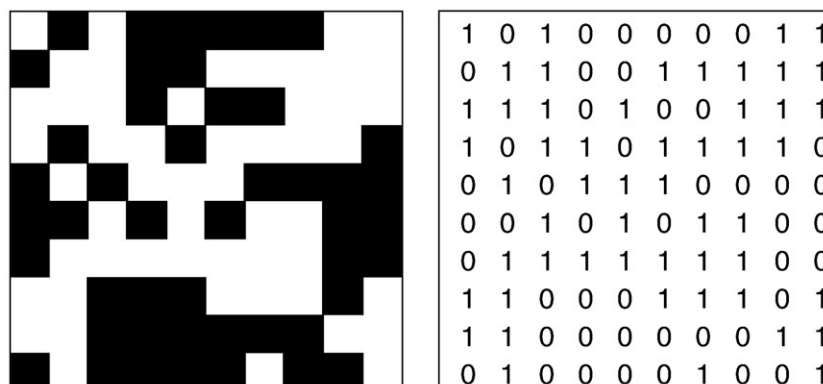


Fig. 1. (a) An example 10×10 random binary map with white boxes representing occupied sites; (b) a binary representation of the same map.

Table 1
Lacunarity calculated for the 10*10 random map in Fig. 1, with a 2*2 (r=2) moving window size

| | S | n [S,r] | Q(S,r) | S*Q(S,r) | S ² *Q(S,r) |
|---------|---|---------|----------------------------|----------|----------------------------|
| r=2 | 0 | 8 | 0.099 | 0.000 | 0.000 |
| N[2]=81 | 1 | 11 | 0.136 | 0.136 | 0.136 |
| | 2 | 27 | 0.333 | 0.667 | 1.333 |
| | 3 | 26 | 0.321 | 0.963 | 2.889 |
| | 4 | 9 | 0.111 | 0.444 | 1.778 |
| | | | Z ⁽¹⁾ =2.209876 | | Z ⁽²⁾ =6.135802 |

S=occupied sites, n[S,r]=number of boxes of size r containing S occupied sites; Q(S,r)=probability of distribution of occupied sites S, with box size r. First moment Z¹ and second moment Z² of the distribution. A[2]=1.256421.

Lacunarity can thus be considered a scale-dependent measure of heterogeneity or texture (Plotnick et al., 1993). While lacunarity was originally developed to describe a property of fractals it can be extended to the description of general spatial patterns, including, but not restricted to those with fractal and multifractal properties (Plotnick et al., 1996).

1.3. Calculation

Allain and Cloitre (1991) presented an algorithm to calculate lacunarity by utilising a moving window. This algorithm is briefly summarised here with the aid of a 10 × 10 random binary map (Fig. 1). First, an r × r box (initially r=2) is placed on the upper left corner. In the case of Fig. 1, the number of occupied sites (white cells) in this 2 × 2 box is two. The box is then displaced by one pixel to the right, and the number of occupied sites again counted (in this case three). The procedure is then repeated by moving the window over the map. If the size of the map is M, and it is squared-shaped, the total number of boxes of size r is N[r]:

$$N[r] = (M - r + 1)^2$$

We can then produce a frequency distribution of the count of white cells (occupied sites) (Table 1). The number of boxes of size r containing S occupied sites is n[S,r]. This frequency

distribution is converted into a probability distribution by dividing by N(r):

$$Q(S, r) = n[S, r]/N[r].$$

We can then calculate the first moment Z⁽¹⁾ and the second moment Z⁽²⁾ of this distribution.

$$Z^{(1)} = \sum S * Q(S, r)$$

$$Z^{(2)} = \sum S^2 * Q(S, r)$$

The lacunarity A depends of the box size r and is defined as:

$$A[r] = Z^{(2)} / [Z^{(1)}]^2$$

Recognising that Z⁽¹⁾=M[r] and that Z⁽²⁾=s_s² [r]+M[r]² where M[r] is the mean and s_s² [r] the variance of the number of sites per box, the lacunarity can be rewritten as:

$$A[r] = s_s^2[r]/M[r]^2 + 1$$

As a result, lacunarity clearly depends not only on the size of the moving window, r, and on the fraction P of the map occupied by the habitat of interest (white squares on the random map) but also on the distribution of the gaps (black squares) in the landscape. Thus, two different maps with the same fraction of occupied sites can have different lacunarities depending on the distribution of their gaps.

1.4. The scale-dependency of lacunarity vs. box size

As lacunarity is clearly a scale-dependent variable, the most useful information is obtained by plotting lacunarity against a range of different moving window sizes, and it has become conventional to present these plots in logarithmic axes. A number of useful parameters can be obtained from such a plot, and these are illustrated in Fig. 2, an example from a tropical rainforest canopy at Caxiuanã, Brazil. The detailed properties of the site will be presented later; here the graph is simply presented as an illustration of the utility of this form of plot.

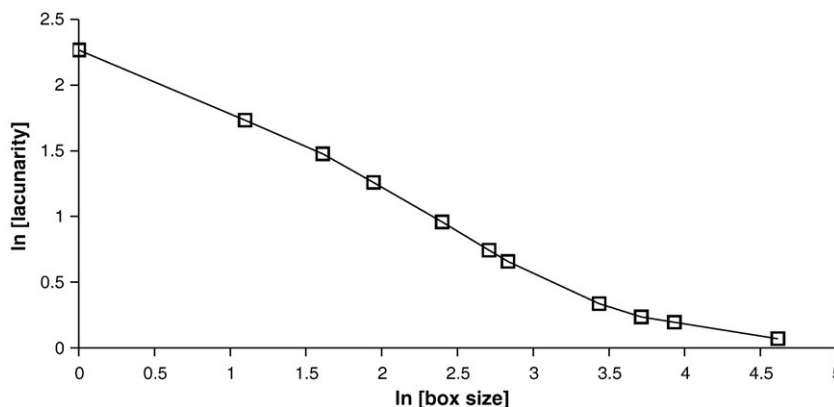


Fig. 2. Example of lacunarity values from a subset of an IKONOS image of a terra firme rainforest at Caxiuanã, Pará, Brazil, plotted against box size. Both axes have been logarithmically transformed.

The y -intercept of each curve is the inverse of the fractional coverage and represents the highest value of lacunarity (the individual pixel is the most inhomogeneous unit in the map). Indeed, for $r=1$ (a moving window equal in size to a pixel), $A[1]=1/P$:

$$Q(1, 1) = P,$$

$$A[1] = Z^{(2)} / [Z^{(1)}]^2 = P/P^2 = 1/P.$$

At small spatial scales, that is, for moving window sizes much smaller than the size of the dominant textural components of the map (e.g. tree crowns and shadows), most boxes are either mostly full or totally empty. As a result, the variance of the number of occupied sites in a moving window, and thus the lacunarity, is high. At large spatial scales (large moving window sizes), the size of the moving window, r , becomes larger than any repeating spatial pattern in the landscape, the variance in the number of occupied sites in the moving window diminishes, and the lacunarity tends to one (and its logarithm tends to zero). The map can be described as being translationally invariant at this scale.

The exact nature of the decline of the lacunarity with increasing scale is perhaps the most interesting aspect of the plot, and reflects the fractal properties of the image. Plotnick et al. (1996) showed how the slopes of lacunarity curves vary in

landscapes with different textural distributions: from random to regular. If the decline in lacunarity is linear (or quasi-linear) over a range of spatial scales then, then the image exhibits self-similar or fractal properties over that range of scales (Manrubia & Solé, 1997; Plotnick et al., 1996; Ricotta et al., 2001; Solé & Manrubia, 1995). At these scales, the slope of the plot (in logarithmic axes) is equal to $F-E$, where F is the fractal dimension, and E is the Euclidean dimension ($=2$ for a planar image) of the object (Allain & Cloitre, 1991). Hence, the extent of self-similarity and the corresponding fractal dimension can be directly calculated from plots such as that shown in Fig. 2.

2. Methods

2.1. Sites

To explore the lacunarity properties in a variety of tropical forest canopies, we used 1 m resolution IKONOS panchromatic images of several Amazon rainforest landscapes, obtained from the Large-Scale Biosphere-Atmosphere Experiment in Amazonia (LBA) data archive (www-eosdis.ornl.gov/lba_cptec/) for Brazil and directly purchased for Peru. Four sites were in Brazil: Caxiuana and Santarem (state of Pará), Sinop (Mato Grosso) and Manaus (Amazonas); and one in Peru: Tambopata (Madre de Dios). The distribution of the sites across Amazonia is shown

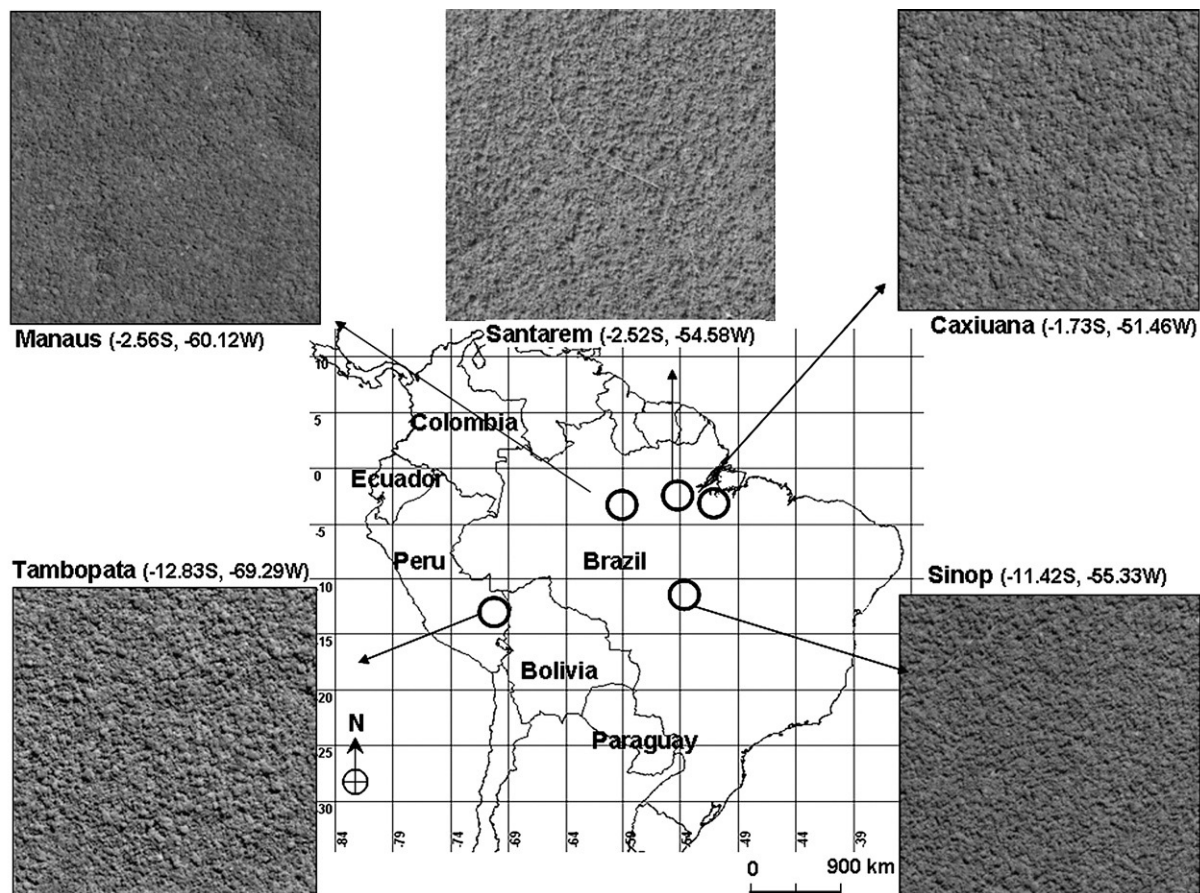


Fig. 3. Distribution of the five study sites across Amazonia, with the IKONOS satellite subset areas at 1-m resolution. These subset areas were selected to include exclusively *terra firme* forests. Coordinates correspond to the center point of the subsets.

Table 2
IKONOS metadata for the five selected Amazonian landscapes (field site and state)

| IKONOS satellite images | Caxiuana-PA | Manaus-AM | Sinop-MG | Santarem-PA | Tambopata-MD |
|-------------------------|------------------|------------------|------------------|------------------|------------------|
| Latitude | −1.78 to −1.71 | −2.62 to −2.56 | −11.44 to −11.38 | −2.88 to −2.82 | −12.89 to −12.80 |
| Longitude | −51.48 to −51.42 | −60.15 to −60.08 | −55.36 to −55.29 | −54.98 to −54.92 | −69.35 to −69.25 |
| Columns | 7004 | 7029 | 7004 | 7020 | 10504 |
| Rows | 7004 | 6989 | 7100 | 6984 | 9504 |
| Sun angle azimuth | 47.02 | 50.47 | 39.96 | 127.05 | 63.38 |
| Sun angle elevation | 52.81 | 57.57 | 49.40 | 68.96 | 66.41 |
| Acquisition date/time | 2000–06–07/13:30 | 2001–08–02/14:24 | 2001–05–19/13:52 | 2001–11–03/14:14 | 2004–09–29/15:04 |

Lacunarity analyses were run on the panchromatic bands of the IKONOS images (1-meter spatial resolution), all in geodetic system (lat/long), WSG84.

in Fig. 3, and the properties of the original IKONOS images are summarized in Table 2. Note that solar elevation angles (and thus angle-dependent shadowing effects) vary through only a moderate range between images, between 49° and 67°. To examine intra-landscape vegetation variation in more detail, we focused in particular on subsets of two images (one in Caxiuana and one in Tambopata) that contained both swamp forest vegetation and *terra firme* tropical forests. These forests differ strongly in composition and structure. The *terra firme* forests are characterized by low nutrient concentrations and well-drained soils (Carvalho et al., 2004). They are typically rich in buttressed trees, a forest canopy that reaches 25–40 m in height, with emergents up to 50–60 m. The understorey is relatively sparse and includes palms, woody vines and vascular epiphytes such as ferns, bromeliads, and orchids. The swamp forest has shorter trees, with narrower crowns and an abundance of palms, and vegetation is adapted to seasonal or permanent flooding. In general, the resulting forests are shorter in stature, have many specialized species of flora and fauna, and relatively low floral diversity. To examine forest properties of these five landscapes we compiled plot data located in the proximities of the selected areas. The location and properties of these forest plots are described in Table 3, together with relevant structural and dynamic variables. All these plots belong to the RAINFOR forest inventory network (Malhi et al., 2002).

2.2. Reclassification of satellite image into a binary map and calculation of lacunarity plots

While lacunarity analysis can be applied to quantitative continuous datasets (Plotnick et al., 1996), the interpretation is simpler for a binary map, and for simplicity of analysis we work here only with binary maps. Therefore, our first step was to reclassify the greyscale IKONOS panchromatic images into binary maps where the brightest pixels were given a value of 1 (occupied cells, bright cells), and the remainder a value of 0 (gaps, dark cells). While the binary approach is a simple, effective and frequently used technique in textural analysis (Plotnick et al., 1996; Solé & Manrubia, 1995; Weishampel et al., 1998, 2001), it should be noted that for spectral conversions, the resulting binary images reduce the information content relative to the original data. Moreover, using a brightness threshold will group image features that relate to different structures into one category (e.g. dark pixels can represent shaded crowns but also ground penetrating gaps).

To examine the sensitivity and robustness of lacunarity analysis to details of the analysis procedure, we tested the effect of different occupancy levels (P) on the final lacunarity values. Hence the greyscale threshold for deciding the brightest pixels (level of occupancy P) was varied so that the total fraction of occupancy was increased between 10% and 90%, in increments of 10% (Fig. 4a,b).

Table 3
Forest structure parameters from one hectare plots in *terra firme* forests within each study region

| <i>Terra firme</i> IKONOS subsets | Caxiuana-PA | Manaus-AM | SINOP-MG | Santarem-PA | Tambopata-MD |
|---|---------------|---------------|----------------|---------------|----------------|
| IKONOS lat/long central point | −1.74, −51.45 | −2.57, −60.10 | −11.42, −55.33 | −2.87, −54.96 | −12.84, −69.32 |
| Forest plot lat/long central point | −1.71, −51.53 | −2.30, −60.0 | −11.41, −55.32 | −2.75, −55.0 | −12.83, −69.27 |
| Year of census | 2003 | 1999 | 2002 | 1995 | 2003 |
| Intercensal period (years) | 3.4 | 7.9 | n/a | 6.0 | 3.1 |
| Number of plots used in calculations | 1 | 4 | 1 | 3 | 1 |
| Tree density (trees ha ^{−1}) | 515 | 547 | 474 | 527 | 531 |
| Fraction of trees with dbh 10–20 cm (%) | 56.1 | 62 | 61.4 | 60.7 | 64 |
| Fraction of trees with dbh >40 cm (%) | 9.5 | 7.7 | 9.8 | 10.2 | 7.0 |
| Total basal area, BA (m ² ha ^{−1}) | 30.6 | 25.6 | 22.4 | 29.7 | 25.1 |
| Fraction of BA with dbh 10–20 cm (%) | 15.3 | 21.0 | 20.8 | 16.3 | 21.7 |
| Fraction of BA with dbh >40 cm (%) | 49.7 | 39.9 | 43.2 | 53.2 | 44.8 |
| Stem recruitment rate (%) | 1.16 | 1.67 | n/a | 1.37 | 1.47 |
| Stem mortality rate (%) | 0.93 | 2.24 | n/a | 0.60 | 3.90 |
| Plot size and shape (m) | 10×1000 | 100×100 | 20×500 | 50×50 | 100×100 |

Forest plot data are from the RAINFOR network database (<http://www.geog.leeds.ac.uk/projects/rainfor/>). When more than one plot was used in the calculations, mean values are given.

Lacunarity was then calculated for each test image using the Allain and Cloitre (1991) algorithm outlined above, with a range of square moving-window sizes varying from $r=1$ pixel (1 pixel=1 m) up to $r=101$ pixels (101 m). The logarithm of lacunarity was plotted against the logarithm of box size, as illustrated in Figs. 2 and 4. Final lacunarities were, therefore, mean values per image, plotted against moving-window size in log-log plots (Fig. 7).

2.3. Production of maps of lacunarity, the index of translational homogeneity, and fractal dimension at the landscape level — scaling up

In addition to creating plots of how total lacunarity varies in a studied area, it would be useful to map how the properties of lacunarity, translational homogeneity or fractal dimension vary across the landscape. To do so, we need to choose a suitable maximum box size for the scaling-up process. There is no single scale or window size that can be prescribed to analyse the complex spatio-temporal patterns and hierarchical structure of heterogeneous forest canopies (Frazer et al., 2005). Therefore, a compromise needs to be struck between a large box size, which

homogenises small-scale information but gives improved statistics in the lacunarity calculation, and small box sizes, which reveal finer-scale information on variation in the landscape, but also increase statistical noise. For our purpose of forest canopy identification, and for our tropical landscapes, a fixed maximum box size of 51×51 pixels (each pixel 1 m) was found to be near this optimum size, being larger than individual tree crowns or gaps, the largest unit of interest. Other landscapes (e.g. sparse vegetation) might require a different maximum box size to adequately map textural properties. In the final map, the metric (e.g. lacunarity) for that 51×51 pixel box was assigned to the pixel at the centre of that box. The box was then displaced one pixel and the analysis repeated, until every pixel within the map is assigned a value, with the exception of those within 25 pixels of the original image boundary. This approach generated maps of lacunarity and fractal dimension.

It would also be useful to define a length scale that defines the point where the log-log lacunarity curve approaches the x -axis, and therefore indicates translational invariance. The first step was to determine the length-scales over which the decline of lacunarity is quasi-linear (and hence the map self-similar), by plotting a linear fit through three consecutive points on the

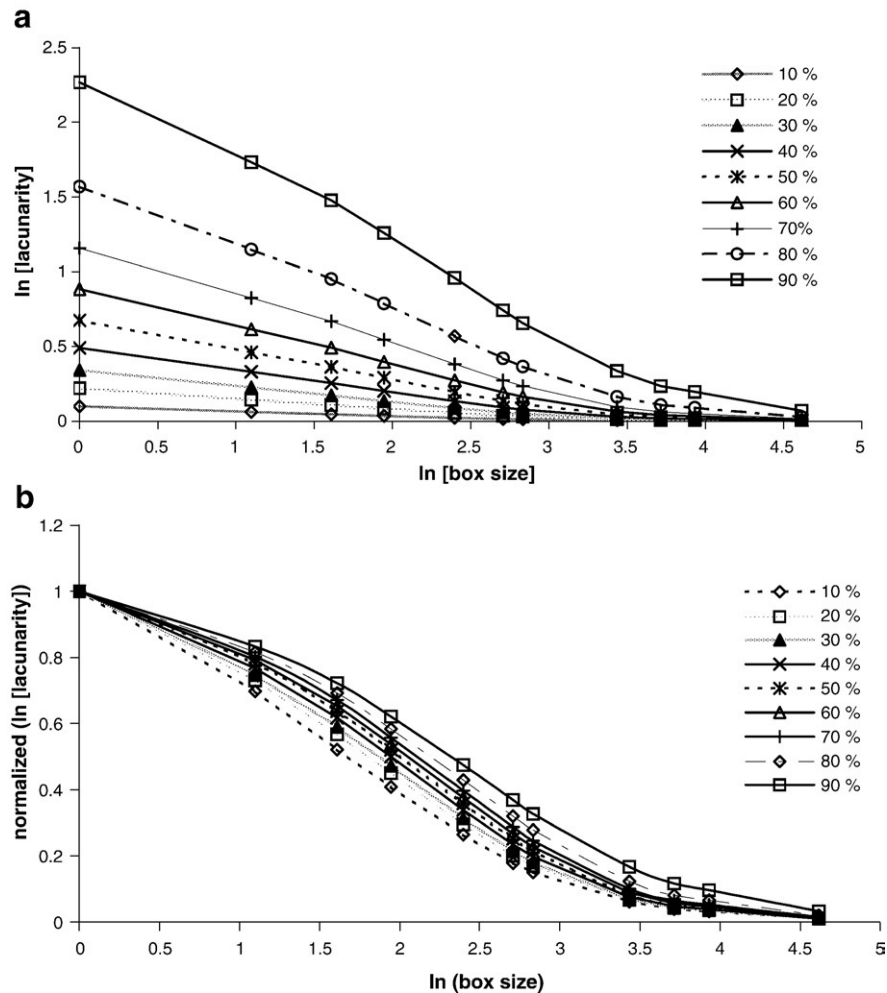


Fig. 4. (a) Lacunarity plotted against box size for different thresholds of pixel occupancy (10%–90%); (b) normalized lacunarity values at different thresholds of pixel occupancy, corresponding to the values of (a) divided by $\ln[A(1)]$; (c) test of the sensitivity of lacunarity to fractional coverage; and (d) normalized values of (c).

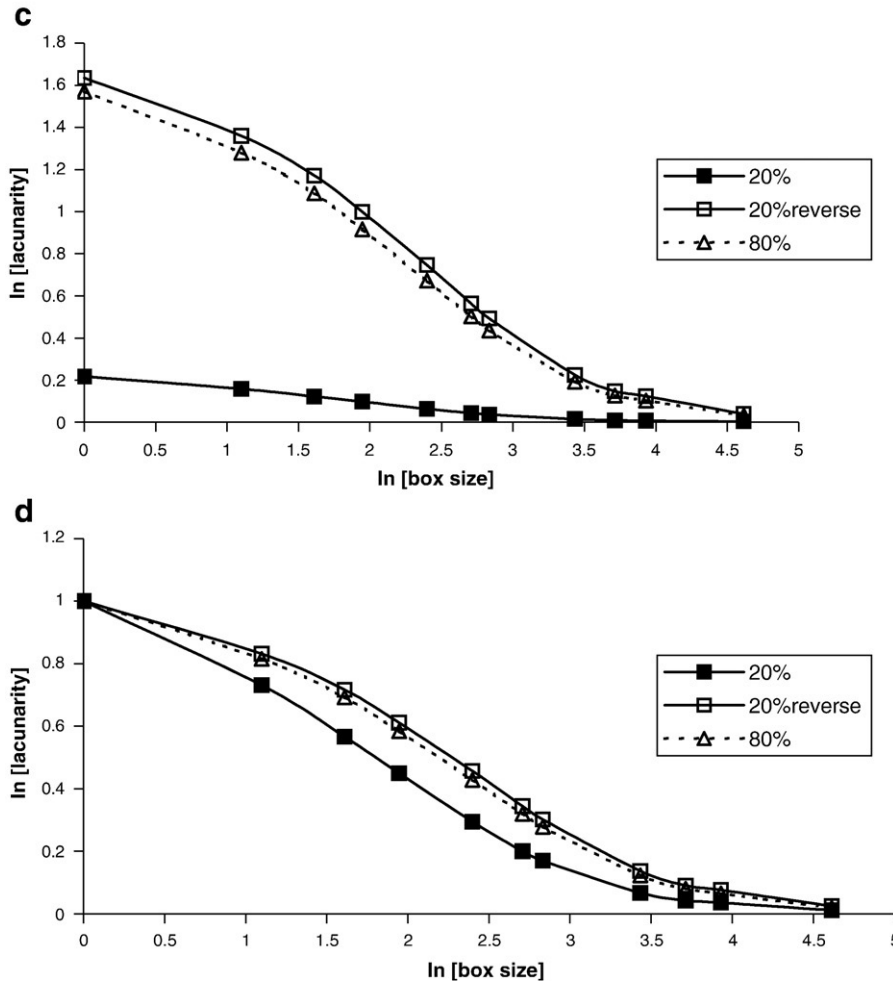


Fig. 4 (continued).

lacunarity curve. If the three points line up, the coefficient of determination, r^2 , of the linear fit approaches 1. Hence the value of r^2 , between 0 and 1, is an indicator of linearity. We plotted the variation of this index of linearity r^2 with increasing length scale and determined the three consecutive box sizes with maximum linearity (e.g. 1–3–5 m, 3–5–7 m, 5–7–11 m, 7–11–15 m, 11–15–17 m), and used this as the basis of our linear interpolation.

Based on the threshold were our forests showed self-similar and scale independent properties, we define the Index of Translational Homogeneity (ITH) as:

$$ITH = \exp \left[\ln(r_{low}) - \frac{\ln(A(r_{low})) * [\ln(r_{high}) - \ln(r_{low})]}{\ln(A(r_{high})) - \ln(A(r_{low}))} \right]$$

where r_{low} and r_{high} define the range of approximate linearity in the lacunarity curve (in our case 5 m and 11 m respectively, see Results section). Thus, the ITH can be visualized as the x -intercept of the linear extrapolation of the linear (self-similar) part of the lacunarity curve. The ITH is a landscape-dependent length scale that refers to a value beyond which there is translational invariance in texture and homogeneity of the canopy structure. When translational homogeneity is reached the values of lacunarity are

independent of the box position. As with the maps of lacunarity and fractal dimension, to generate the ITH maps at a landscape level, the ITH values were resampled with a moving window of 51×51 m that allocated a single ITH value for the central pixel of each window box.

2.4. Variation of lacunarity and associated properties within a landscape

We would expect lacunarity properties to vary among distinct forest types in a landscape. To test this assumption, we examined the variation of lacunarity within an IKONOS image of the Caxiuanã forest canopy (extracted from the panchromatic band, Table 2) (Fig. 5a). The chosen subset of the image covered an area of well-drained *terra firme* forest (TF), and poorly drained swamps ($551 \text{ m} \times 344 \text{ m}$). A fractional occupancy value of $P=50\%$, and a maximum moving window of 51×51 -meters were chosen for all the analyses.

Together with the visual interpretation of the above variables, we plotted the mean lacunarity values for different box sizes, both for the Caxiuanã IKONOS subset, and for a Tambopata subset ($1816 \times 1417 \text{ m}$). We then calculated mean ITH values for the *terra firme* and swamp vegetation types, for

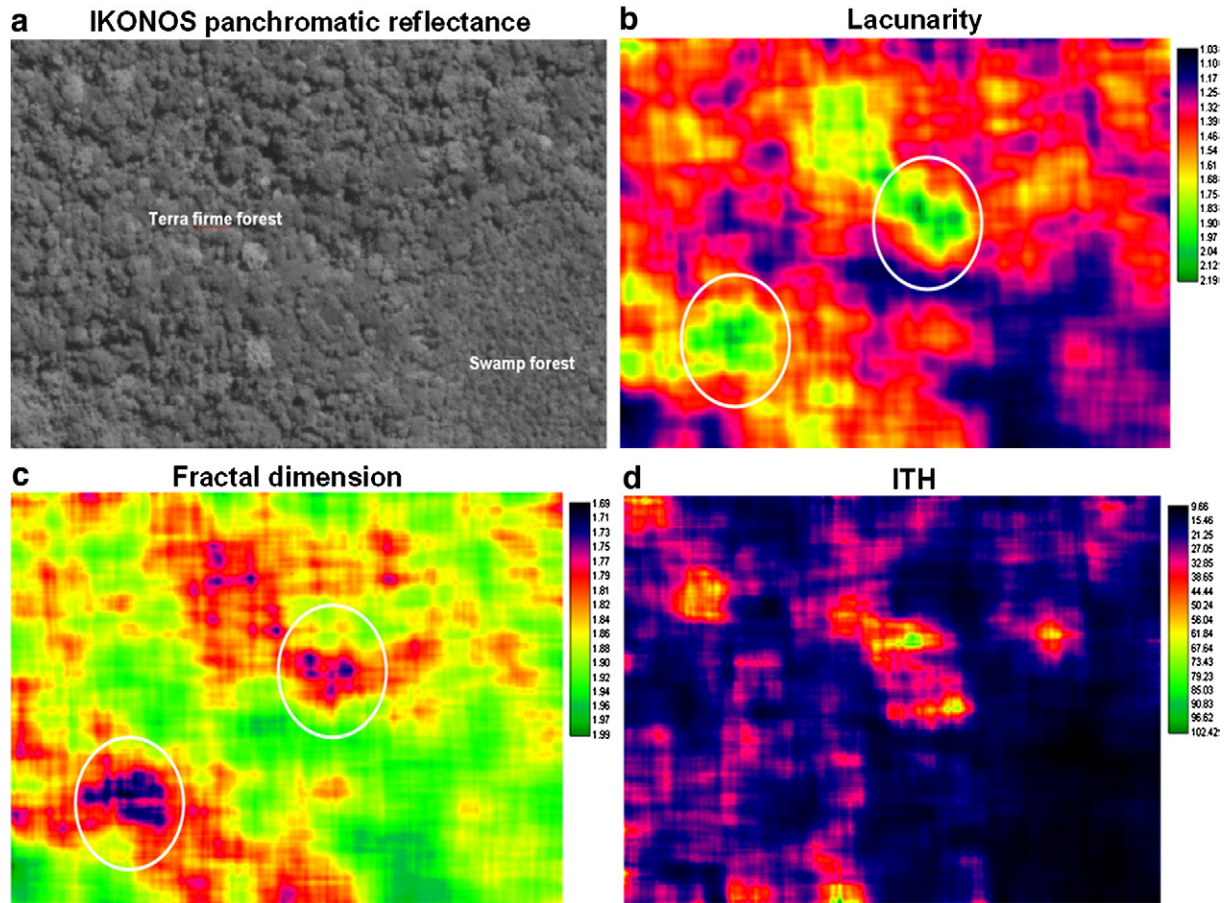


Fig. 5. (a) Panchromatic band IKONOS image of the Caxiuaná IKONOS forest, at 1 meter spatial resolution; (b): lacunarity map of the above; (c): fractal dimension map; and (d) Index of Translational Homogeneity (ITH) map. All analyses were based on a 51×51 -meter moving window, and a 50% level of occupancy.

Caxiuaná and Tambopata, following the procedure explained above (i.e. interpolation of the imaginary line that connects $r=5$ m and $r=11$ m, until crossing the x -axis, where $\ln(A)=0$). All analyses were performed using Idrisi Kilimanjaro GIS software (Clark Labs, USA).

2.5. Variation of lacunarity and associated properties among Amazonian sites

We compared the heterogeneity of gap distribution and ITH values among the five Amazonian sites (Fig. 3), exclusively concentrating on areas with *terra firme* vegetation, so that any differences indicated different structural properties of the canopy that were independent of forest type. Subsets were created of the original panchromatic IKONOS images covering approximate areas of 1000×1000 m (Table 2). The final outcome was a raster of ITH variations within each landscape. To assist visual comparisons, the final ITH values were classified into 10 categories: 1: 0–19 m, 2: 20–29 m, etc, 9: 90–99 m, 10: > 100 m. Lacunarity vs. length scale curves for each analysed 1000×1000 m subset were also generated.

2.6. Comparison of ITH with manual estimation of crown size

To evaluate the accuracy of the spatial distribution of ITH values, we selected at least three subtiles of 100×100 m each

inside the subsets of *terra firme* for all sites (Caxiuaná, Santarem, Sinop, Manaus and Tambopata). In each subtile, we visually estimated the maximum diameter of all distinguishable tree crowns (ca. 150 trees per subtile) and calculated a manually-derived mean crown size. We then extracted the area of these subtiles and obtained a raster with the spatial distribution of ITH. For each of these subtiles rasters, the mean values of ITH were calculated plotted against mean crown size. Similar analyses were run for swamp areas in Tambopata and Caxiuaná.

3. Results and discussion

3.1. Sensitivity of lacunarity to analysis procedure

Fig. 4a illustrates how the lacunarity plots vary with increasing greyscale thresholds in the binary maps, with higher vertical intercept values as occupancy P increases. Normalization of the curves by division by $\ln[A(1)]$ enables direct comparison among curves (Fig. 4b). After normalization, low occupancy ($P=10\%$) binary maps have lower lacunarity (less gappiness) than higher occupancy maps (e.g. $P=90\%$), but differences are relatively small.

Overall, the canopy appears self-similar on scales between 3 m and 30 m ($\ln(3)=1.15$ and $\ln(30)=3.4$), indicated by the quasi-linear decrease in the lacunarity plot. Above 30 m the canopy shows translational homogeneity. This makes intuitive

sense; 30 m corresponds to the crown size of medium-large canopy trees. Below this length scale (<30 m), the architecture of individual trees shows some elements of self-similarity; above this scale the randomness of tree position and canopy size introduces a tendency towards spatial invariance (see also Fig. 8 later).

The variation of the shape of the normalized curve with occupancy, P , is interesting. Does it reflect a geometrical property of the canopy surface, or does it simply show a sensitivity of lacunarity to P ? This was tested by reversing the binary code (i.e. 1 becomes 0, 0 becomes 1), as shown in Fig. 4c. The 20% reverse map, i.e. the darkest 20% of pixels (coded 1) had the same lacunarity curve as the 80% map, i.e. brightest 20% of pixels (coded 0). This symmetry in lacunarity properties indicates that low occupancy maps have innately smaller scales of translational homogeneity than high occupancy maps, i.e. the index of translational homogeneity varies with fractional occupancy. Hence a fixed threshold of occupancy needs to be chosen when comparing images. This also overcomes the need to normalize the graphs, as all maps with the same occupancy levels will have the same vertical intercepts, allowing curve comparisons. In order to compare images, and for the rest of the paper, an occupancy fraction of 50% was chosen.

3.2. Variation of lacunarity and associated properties within a landscape

The swamp forest canopy appears more “fine-grained” than the *terra firme* forest, indicating a preponderance of palms and other small-crowned trees (Fig. 5a). The lacunarity is explicitly mapped in Fig. 5b (for maximum box size 51 m). The contrasts between the swamp vegetation and *terra firme* forest are evident, as is the presence of a tongue of swamp forest extending westwards, corresponding to a small stream tributary. Perhaps more surprising is the presence of large contrasts of lacunarity within the *terra firme* forest; inspection of Fig. 5a suggests that high lacunarity areas are those with larger tree crowns, and perhaps emergent trees casting shadows over the forest canopy. Hence this textural analysis brings to the fore subtle variations in canopy texture.

The fractal dimension is mapped in Fig. 5c. In this map, it appears fractal dimension mainly reflects occupancy by dark pixels and is thus sensitive to shadow fraction rather than representing any fundamental geometric property of the canopy. The fractal dimension is lower in many of the areas corresponding to high lacunarity forests in Fig. 5a, although it also picks out other shadow-rich areas that do not correspond to large crown size.

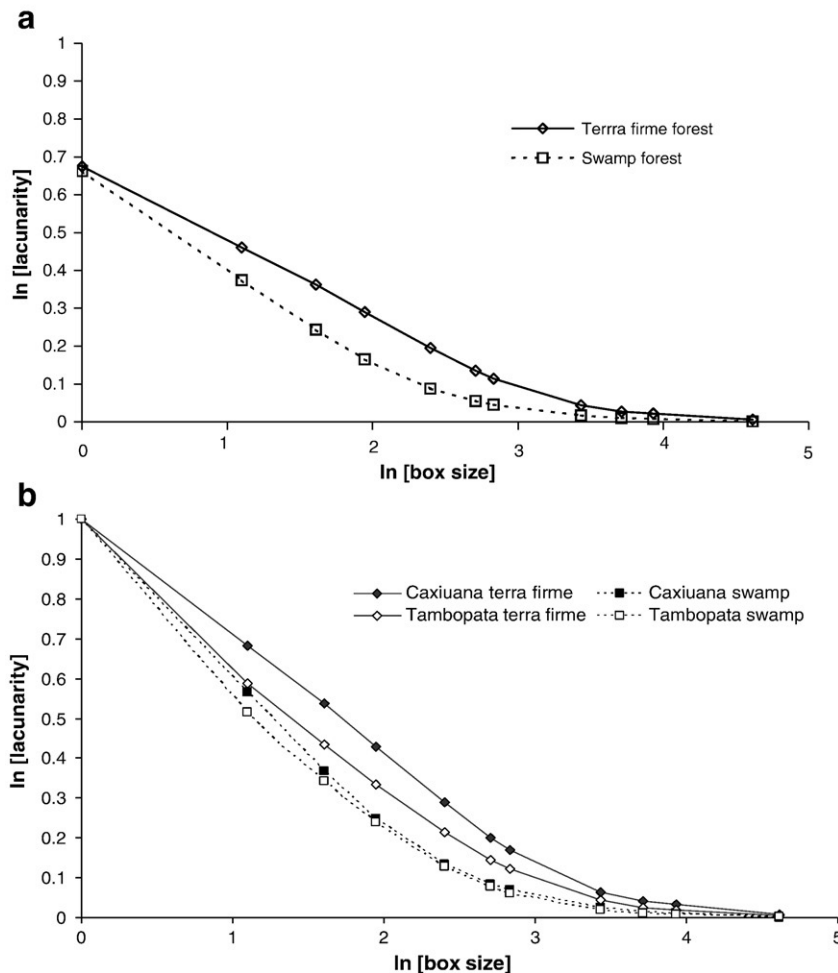


Fig. 6. Lacunarity plots for terra-firme and swamp forest in (a) Caxiuana, Brazil; (b) Tambopata, Peru.

The index of translational homogeneity (ITH) is mapped in Fig. 5d. This is the most useful map, as it combines information from the (scale-dependent) map of lacunarity and the (shadow dependent) map of fractal dimension to produce information that has an obvious interpretation, and that is potentially less dependent on both scale and shadow fraction. The ITH has values of about 10–15 m in the swamp vegetation, and this rises to 50–60 m in some areas of *terra firme*, but can be as low as 15–20 m in other areas of *terra firme*.

The contrast between large-crowned *terra firme* forest and small-crowned swamp forest is obvious, but the differences between different areas of *terra firme* are worth exploring. Note the properties of the area next to the bottom left of the map, which has high lacunarity, but high shadow fraction (low fractal dimension) and a small ITH. Hence, the high lacunarity is caused by the high shadow fraction, despite the fact that crown sizes are relatively small. In contrast, the area in the upper center has large tree crowns but a slightly lower shadow fraction, and thus both high lacunarity and high ITH. The bottom left area

indicates an area of medium-size tree crowns, but rough or gappy forest canopy. The upper center area indicates an area of large tree crowns. The swamp forest is an area of medium-small tree-crowns but closed canopy with low shadow fraction.

The visual and lacunarity differences between swamp vegetation and *terra firme* forests observed in Fig. 5a and b, were confirmed by the lacunarity plots for these two ecosystems in Caxiuana (Fig. 6a). Both forest canopies show self-similarity at small scales (the lacunarity curves are fairly straight over an order of magnitude of box sizes [$\ln(r)$ ranging between 1 and 2.5]) but the slope of the curve is steeper for the swamps (i.e. the fractal dimension is smaller for the swamp forest). The rate of decline in lacunarity with box size depends on the presence and heterogeneity of coarser-scale patterns (Frazer et al., 2005), with slow declining plots suggesting the occurrence of larger-scale aggregation patterns.

To investigate the spatial value at which uniformity is reached, we calculated the ITH from Fig. 6b by a linear extrapolation of lacunarity values at $\ln(3)$ and $\ln(7)$ as described

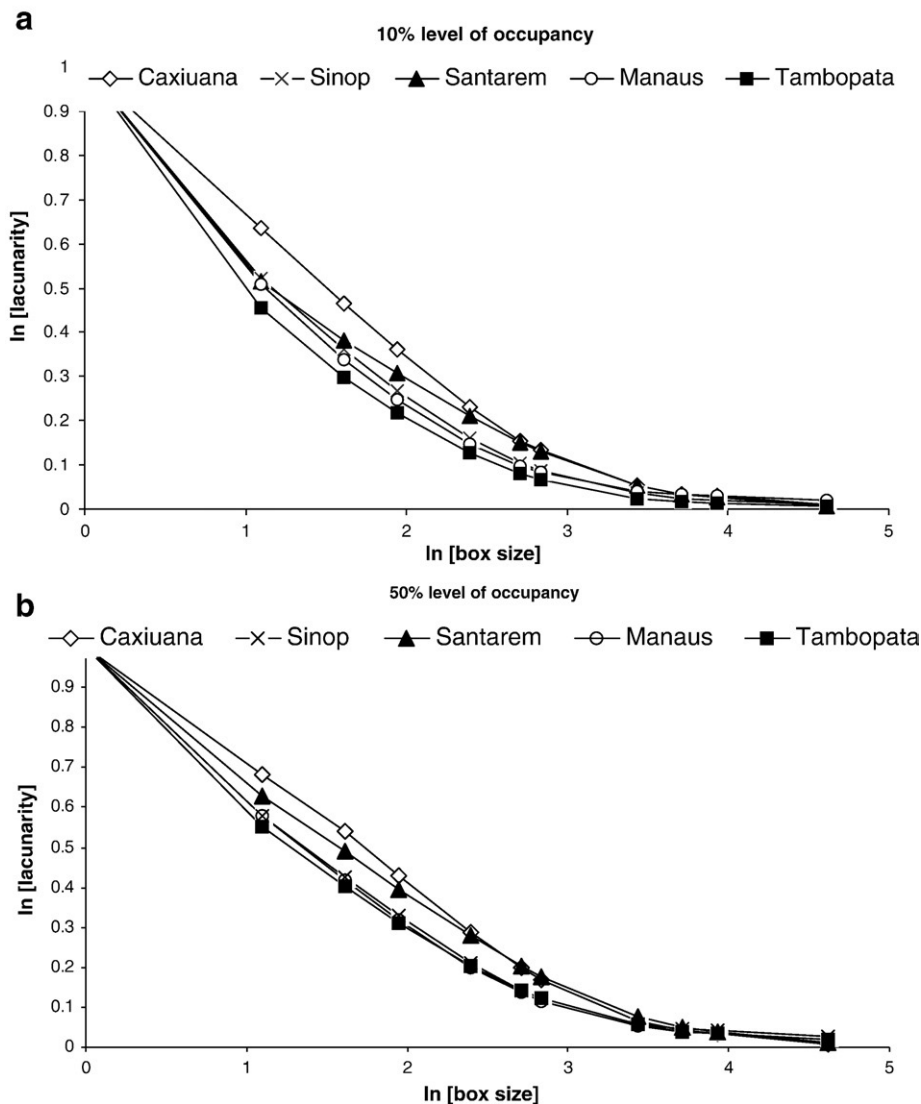


Fig. 7. Normalized lacunarity plots for different *terra firme* forest canopies across Amazonia, with (a) 10% level of occupancy (P), and (b) 50% level of occupancy (P).

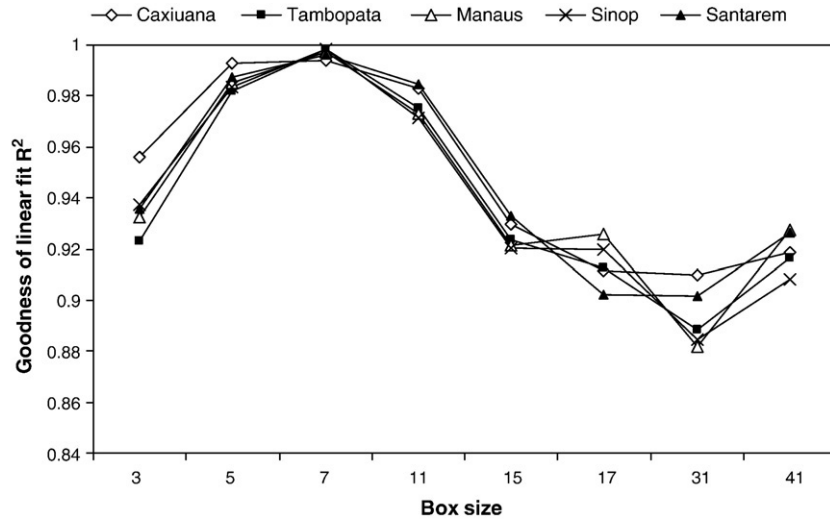


Fig. 8. Variation of self-similarity with length scale, for different *terra firme* forests. Each graph represents the goodness of fit (R^2) of a linear fit to three consecutive points on the lacunarity curve (e.g. box sizes [1,3,5], [3,5,7], [5,7,11],[7,11,15] m). Maximum linearity occurs at $r=1.9$ [$\ln(7)$]. Between $r=5$ m and $r=11$ m the lacunarity curve is almost linear and the forest canopy image is self-similar and exhibits fractal properties.

above. This gives scales of translational homogeneity of 29.5 m (exp (3.4)) and 13.6 m (exp (2.6)) for *terra firme* and swamp regions respectively. Because of the concavity of the lacunarity curves, the linear interpolation of the plot tends to slightly underestimate the true scale of translational homogeneity obtained in the map.

Fig. 6b shows the differences between swampy vegetation and *terra firme* at two extreme positions in the Amazon

gradient: the eastern site at Caxiuana (Brazil) and western site in Tambopata (Peru). For both sites, lacunarity values for *terra firme* forests are consistently higher than lacunarity values for the swamp vegetation. For the same level of occupancy and the same box size, higher lacunarity values for *terra firme* indicate a more clustered distribution of the objects (Plotnick et al., 1996). This greater clumping might be enhanced by the presence of canopy shadows that do not exist in the finer-

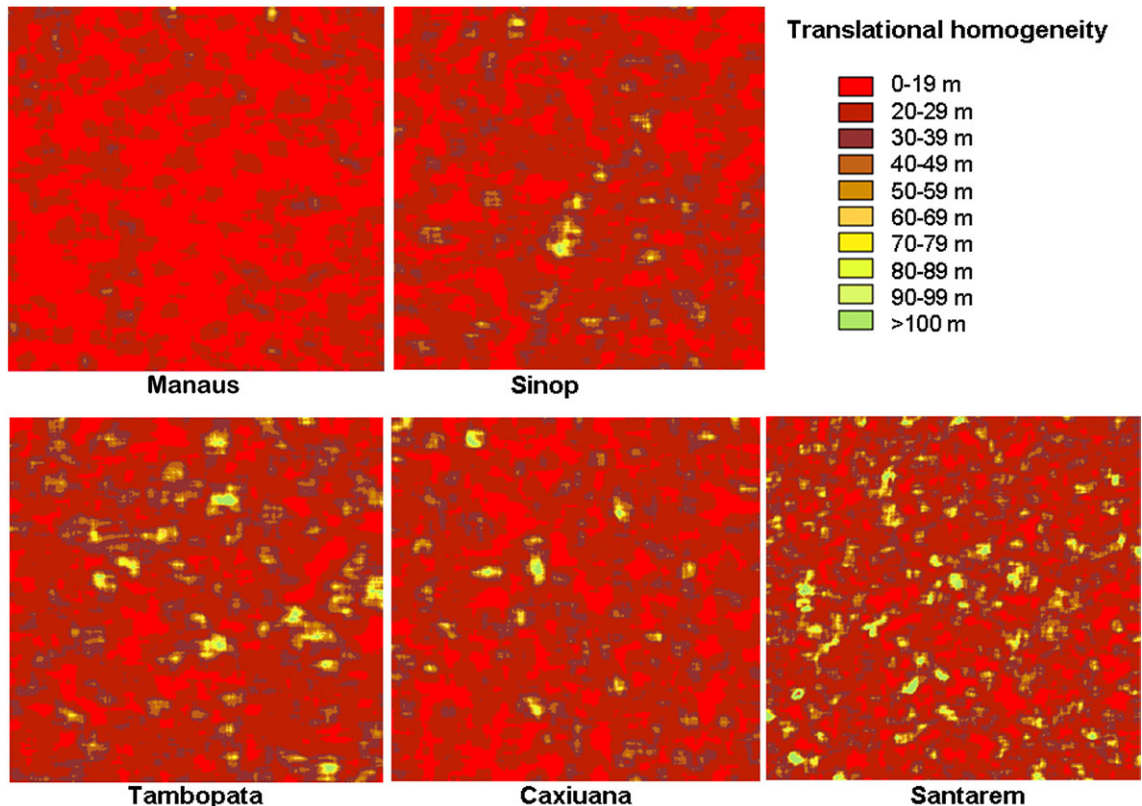


Fig. 9. Maps of ITH for image subsets of *terra firme* forests in the five study regions.

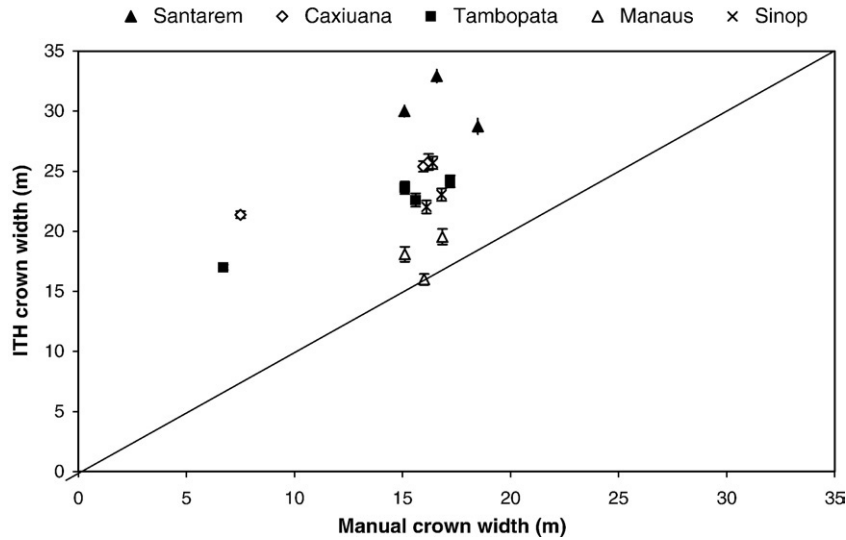


Fig. 10. Plot of the index of translational homogeneity against manually-calculated mean crown width (meters).

grain swampy vegetation. The convergence of lacunarity plots for swamp vegetation above a scale of $r=7$ m ($\ln(r)=1.94$) suggests that for scales larger than 7 m, both Caxiuana’s and Tambopata’s swamps have very similar textural properties.

Linear interpolations of the plots to detect the translational homogeneity scales indicate lower values for Tambopata than for Caxiuana in the case of *terra firme* (23.3 vs 29.5 m), indicating larger crowns in Caxiuana, while there is little difference in the swamp areas (15.6 vs 13.7 m, Tambopata and Caxiuana respectively).

3.3. Variation of lacunarity and associated properties among Amazonian sites

Fig. 7a and b display the normalized mean lacunarity values for all sites, at 10% and 50% levels of occupancy. 10% occupancy fraction plots distinguish better between sites, whereas the distribution of gaps in the landscape at 50% occupancy is more homogeneous for central and western Amazonian sites (Manaus, Sinop and Tambopata). The highest lacunarity values are found at the eastern Amazonian site of Caxiuana.

For a given P , higher lacunarity represents higher contagion (fewer but larger gaps; Plotnick et al., 1996). Recent studies of biomass and productivity gradients in the Amazon (Malhi et al., 2004, 2006) reveal that there are marked relationships between these two variables along east-west gradients, with eastern *terra firme* forests being less productive but having higher biomass than western sites. The higher biomass in the eastern rainforests is reflected in forest structural properties (larger tree heights, mean tree sizes, crown sizes, more emergent trees) that can form fewer but larger gaps, and can also cast larger crown shadows.

At $P=50\%$, the plots are quasi-linear for a larger range of box sizes than at $P=10\%$. This improvement of the self-similarity properties of the landscapes at a higher level of occupancy is related to the relative increase of lacunarity for the central and western sites. A linear extrapolation of lacunarity values at $r=3$ m and $r=7$ m to cross the x -axis gives scales of

translational homogeneity of ca. 30 m (exp (3.4) for the eastern sites (Caxiuana and Santarem) and ca. 22 m (exp (3.1) for the other sites.

Fig. 8 displays the variation of self-similarity with length-scale in *terra firme* forest canopies in all five study regions. Peaks of self-similarity (i.e. linearity in Fig. 7) were reached at length scales of 5–11 m for all landscapes, with the exception of Caxiuana that showed linearity in a wider range (3–11 m). Within these thresholds, canopy images showed fractal (self-similar) properties, corresponding to the architecture and arrangement of branches and leaves within individual crowns. Forests have long been characterized as possessing scale-invariant, self-similar features for certain spatial thresholds (Solé & Manrubia, 1995; Sugihara & May, 1990).

Fig. 9 shows the spatial distribution of ITH for the five selected Amazonian *terra firme* landscapes. Santarem and Tambopata showed the highest proportions of high ITH values, and Manaus the lowest. In previous sections we have seen how

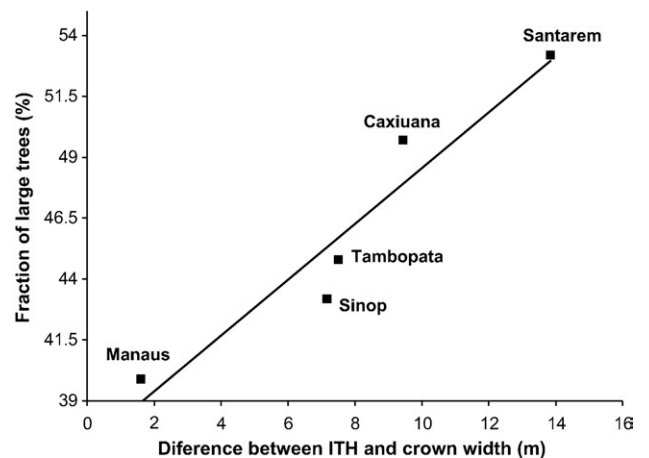


Fig. 11. Plot of the difference between ITH and mean crown width, against the fraction of basal area found in large trees (>40 cm dbh) within a forest census plot from the region of the image.

ITH values of mixed ecosystems (swamp and *terra firme*) followed variations in canopy sizes. In the case of *terra firme* landscapes, we would ideally expect ITH changes to describe heterogeneity in canopy properties, either related to shadows cast by emergent crowns or to the existence of canopy gaps.

If emergent crowns are the major cause of high ITH values, we would expect sites with the highest fraction of large trees (Santarem and Caxiuana; see Table 3) to have the greatest number of high ITH sites. If canopy gaps are the major determinant of high ITH values, we may expect that sites with highest tree mortality rates (Tambopata; Table 3) to have the greatest number of ITH sites. The fact that both Tambopata and Santarem have the greatest density of high ITH sites (Fig. 9) suggests that both these factors are important. However, there is substantial evidence that the Santarem region experienced high levels of mortality in the 1990s prior to forest plot establishment, and this may still be reflected in canopy gap abundance at this site. Thus, canopy gap frequency may be the strongest driver of the incidence of high ITH sites.

3.4. The relationship between ITH and forest canopy properties

The number of high ITH sites may indicate the frequency canopy gaps, but the mean value of ITH within an image may be expected to be more related to mean crown size. Fig. 10 plots ITH against manual estimates of mean crown size for 100 × 100 m subtiles of the IKONOS images. Within any one image, there appears to be a good linear relationship between ITH and mean “observed” (manually calculated) crown size as one moves from small-crowned swamp vegetation to large-ground *terra firme* vegetation (for the Tambopata and Caxiuana images). This confirms that ITH-derived crown values are sensitive to changes in crown size. However, the ITH-derived values are consistently larger than the manually calculated mean crown sizes.

Considering only the *terra firme* forests in Fig. 10, there is little variation in the “observed” (manually calculated) mean crown sizes between sites. However, for each subtile, the ITH-derived crown value can differ from the “observed” value up to 15 m, being always greater in the ITH-derived values. Clark et al. (2004) reported a good correlation between the IKONOS manual measurements of tree crowns and their values measured in the field at La Selva, Costa Rica. Therefore, we can deduce that our ITH values are over-estimating the real crown values. The magnitude of the offset between ITH and crown size is proportional to the fraction of basal area found in large trees (trees > 40 cm dbh; Table 3), as illustrated in Fig. 11. A likely mechanism is that large trees generate distinct shadows on the surrounding canopy, and the scale of translational invariance observed in the image increasingly shifts to that of crown-shadow combinations, rather than just crowns. Solar elevation angle appears to have little influence on these results, over the moderate range of solar elevations represented in the IKONOS images.

4. Conclusions

We have shown that mean ITH is an indicator of two properties of the tropical forest canopy: (i) mean crown size;

and (ii) heterogeneity of the canopy topography, as represented by the proportion of large trees and their cast shadows. As such, ITH may also be influenced by solar elevation angles at low solar elevations. The high end tail of the distribution ITH values may also be an indicator of canopy gap structure, although this is more speculative.

This research offers insights on an easy technique that can improve our understanding on the spatio-temporal distributions of forest structural and dynamic variables (i.e. mean crown size, presence of emergent trees and gap fractions). ITH maps could therefore be used as proxies for other ecologically variables that are intrinsically related to forest canopy structure, such as forest succession, surface-atmosphere energy and momentum transfer, land use activities such as selective logging (Asner et al., 2005), and forest disturbances such as fire or blowdowns, etc.

A number of studies of Amazonian forests indicate that old-growth tropical forests are undergoing changes in dynamism (Phillips, 1994; Phillips et al., 2004), composition (Laurance et al., 2005) and liana abundance (Phillips et al., 2002; Wright 2005). These changes are likely to influence the textural properties of forest canopies, but the exact relationships between dynamism and forest structure, and between forest structure and textural properties, remain unclear. Conversely, changes in forest textural properties as seen in satellite images can be detected over wide areas and in remote regions, and may therefore be useful indicators of the spatial extent of change.

Indeed, Weishampel et al. (2001) suggested that the increase in lacunarity observed in Landsat images is indicative of such a phenomenon (it should be noted that the analysis presented here operates at scales finer than the pixel size of Weishampel’s analysis, and thus does not offer a ready interpretation of their findings). Lacunarity analysis and ITH may be useful tools for documenting such changes, and we hope that the research presented here provides some guidelines of interpretation of changes in lacunarity and ITH in high resolution images that may be observed in future analyses.

Acknowledgements

The work presented here was conducted as part of LBA (Large-Scale Biosphere-Atmosphere Programme in Amazonia). Special thanks to David Brocas for the initial creation of macros and project development. We also thank Michael Palace, Michael Keller, and Bruce Malamud for useful interaction and comments. YM was supported by a Royal Society University Research Fellowship, and by the Jackson Foundation. RMRC was supported by a Spanish Ministry of Education research grant.

References

- Allain, C., & Cloitre, M. (1991). Characterizing the lacunarity of random and deterministic fractal sets. *Physical Review Annals*, *44*, 3552–3558.
- Asner, G., Knapp, D., Broadbent, E., Oliveira, P., Keller, M., & Silva, J. (2005). Selective logging in the Brazilian Amazon. *Science*, *310*, 480–482.
- Carvalho, J., Silva, J., & Lopes, L. (2004). Growth rate of a *Terra firme* rain forest in Brazilian Amazonia over an eight-year period in response to logging. *Acta Amazonica*, *34*, 209–217.

- Clark, D., Read, J., Clark, M., Murillo, A., Fallas, M., & Clark, D. (2004). Application of 1-m and 4-m resolution satellite data to ecological studies of tropical rain forests. *Ecological Applications*, *14*, 61–74.
- Frazer, G., Wulder, M., & Niemann, O. (2005). Simulation and quantification of the fine-scale spatial pattern and heterogeneity of forest canopy structure: a lacunarity-based method design for analysis of continuous canopy heights. *Forest Ecology and Management*, *214*, 65–90.
- Gefen, Y., Meir, Y., & Aharony, A. (1983). Geometric implementation of hypercubic lattices with noninteger dimensionality by use of low lacunarity fractal lattices. *Physical Review Letters*, *50*, 145–148.
- Huete, L., Didan, K., Miura, T., Rodríguez, E., Gao, X., & Ferreira, L. (2002). Overview of the radiometric and biophysical performance of the MODIS vegetation indices. *Remote Sensing of Environment*, *83*, 195–213.
- Laurance, W., Oliveira, A., Laurance, S., Condit, R., Nascimento, H., Andrade, A., et al. (2005). Late twentieth-century trends in tree-community composition in an Amazonian forest. In Y. Malhi, & O. Phillips (Eds.), *Tropical forests and global atmospheric change* (pp. 97–106). Oxford: Oxford University Press.
- Lewis, S., Malhi, Y., & Phillips, O. (2004). Fingerprinting the impacts of global change on tropical forests. *Philosophical Transactions of the Royal Society of London, Series B*, *359*, 337–462.
- Malhi, Y., Baker, T., Phillips, O., Almeida, S., Alvarez, E., Arroyo, L., et al. (2004). The above-ground coarse wood productivity of 104 Neotropical forest plots. *Global Change Biology*, *10*, 563–591.
- Malhi, Y., Phillips, O., Lloyd, J., Baker, T., Wright, J., Almeida, S., et al. (2002). An international network to monitor the structure, composition and dynamics of Amazonian forests (RAINFOR). *Journal of Vegetation Science*, *13*, 439–450.
- Malhi, Y., Wood, D., Baker, T., Wright, J., Phillips, O., Cochrane, T., et al. (2006). The regional variation of aboveground live biomass in old-growth Amazonian forests. *Global Change Biology*, *12*, 1–32.
- Mandelbrot, B. B. (1983). *The Fractal Geometry of Nature* (pp. 37–56). New-York: W. H. Freeman and Company.
- Manrubia, S., & Solé, R. (1997). On forest spatial dynamics with gap formation. *Journal of Theoretical Biology*, *187*, 159–164.
- Palace, M., Keller, M., Asner, G., Hagen, S., & Braswell, B. (in press). Amazon forest structure from IKONOS satellite data and the automated characterization of forest canopy properties. *Biotropica*. doi:10.1111/j.1744-7429.2007.00353.x
- Phillips, O. (1994). Increasing turnover through time in tropical forests. *Science*, *263*, 954–958.
- Phillips, O., Baker, T., Arroyo, L., Higuchi, N., Killeen, T., Laurance, W., et al. (2004). Pattern and process in Amazon tree turnover, 1976–2001. *Philosophical Transactions of the Royal Society of London. Series B*, *359*, 381–407.
- Phillips, O., Martinez, R., Arroyo, L., Baker, T., Killeen, T., Lewis, S., et al. (2002). Increasing dominance of large lianas in Amazonian forests. *Nature*, *418*, 770–774.
- Plotnick, R., Gardner, R., Hargrove, W., Prestegard, K., & Perlmutter, M. (1996). Lacunarity analysis: a general technique for the analysis of spatial patterns. *Physical Review E, Part B*, *53*, 5461–5468.
- Plotnick, R., Gardner, R., & O' Neill, R. (1993). Lacunarity indices as measures of landscape texture. *Landscape Ecology*, *8*, 201–211.
- Ricotta, C., Arianoutsou, M., Diaz-Delgado, R., Duguay, B., Lloret, F., Maroudi, E., et al. (2001). Self-organized criticality of wildfires ecologically revisited. *Ecological Modelling*, *141*, 307–311.
- Solé, R., & Manrubia, C. (1995). Are rainforests self-organized in a critical state? *Journal of Theoretical Biology*, *173*, 31–40.
- Sugihara, G., & May, R. (1990). Nonlinear forecasting as a way of distinguishing chaos from measurement error in time series. *Nature*, *344*, 734–741.
- Toan, T., Quegan, S., Woodward, I., Lomas, M., Delbart, N., & Picard, G. (2004). Relating radar remote sensing of biomass to modelling of forest carbon budgets. *Climatic Change*, *67*, 379–402.
- Weishampel, J., Godin, J., & Henebry, G. (2001). Pantropical dynamics of intact rain forest canopy texture. *Global Ecology and Biogeography*, *10*, 389–397.
- Weishampel, J., Sloan, J., Boutet, J., & Godin, J. (1998). Mesoscale changes in textural pattern of “intact” Peruvian rainforests (1970s–1980s). *International Journal of Remote Sensing*, *19*, 1007–1014.
- Wright, J. (2005). Tropical forests in a changing environment. *Trends in Ecology and Evolution*, *20*, 553–560.
- Wulder, M., & Franklin, S. (2004). *Methods and Applications for Remote Sensing of Forests: Concepts and Case Studies* (pp. 335–489). Boston: Kluwer Academic Publishers.